1992

Finite thermal diffusivity at onset of convection in autocatalytic systems: Continuous fluid density

Joseph W. Wilder

Boyd F. Edwards

Desiderio A. Vasquez

2-1992

Finite Thermal Diffusivity at Onset of Convection in Autocatalytic Systems: Continuous Fluid Density

J. W. Wilder

Boyd F. Edwards
Utah State University

D. A. Vasquez

Finite thermal diffusivity at onset of convection in autocatalytic systems: Continuous fluid density

Joseph W. Wilder
Department of Mathematics, West Virginia University, Morgantown, West Virginia 26506

Boyd F. Edwards and Desiderio A. Vasquez
Department of Physics, West Virginia University, Morgantown, West Virginia 26506
(Received 6 November 1990; revised manuscript received 3 October 1991)

The linear stability of exothermic autocatalytic reaction fronts is considered using the viscous thermohydrodynamic equations for a fluid with finite thermal diffusivity. For upward front propagation and a thin front, the vertical thermal gradient near the front is reminiscent of the Rayleigh-Bénard problem of a fluid layer heated from below. The problem is also similar to flame propagation, except that here the front propagation speed is limited by catalyst diffusion rather than by activation kinetics. For small density changes in a laterally unbounded system, the curvature dependence of the front propagation speed stabilizes perturbations with short wavelengths $\lambda < \lambda_c$, whereas long wavelengths are unstable to convection. The critical wavelengths λ_c are calculated and compared with experiments and with theoretical results for a similar problem that is driven by a Rayleigh-Taylor instability arising from a discontinuous density difference at the reaction front.

PACS number(s): 47.20.Bp, 47.25.Ae, 03.40.Gc

I. INTRODUCTION

Autocatalytic reaction fronts are of interest in many fields. In systems such as iodate-arsenous-acid mixtures, the front converts unreacted fluid at one density into a reacted fluid at a different density. This conversion results in the release of heat due to the exothermic nature of the reaction. Experimental work on such systems [1] has demonstrated the existence of fronts with constant curvature, moving at constant speeds. The curvature of these fronts is due to the presence of steady convective fluid motion near the reaction front. The convective motion is due to the hydrodynamic instability of the system. The instability may arise from either or both of the following sources. (1) The instability may be caused by the density difference between the reacted and unreacted fluids. With the arsenous-acid system, the reacted fluid has a lower density than the unreacted fluid if measured at the same reference temperature. When ascending fronts are considered, this density difference results in the lighter (reacted) fluid being below the heavier (unreacted) fluid, setting up an instability which is similar to the classical Rayleigh-Taylor instability. (2) The hydrodynamic instability can also be caused by thermal effects. Since the chemical reaction is exothermic, the front is the location of what can be considered to be a heat source. When upward propagating fronts are considered, this heat source results in the fluid far below the front being at a higher temperature than the fluid far above the front. If the temperature difference is large enough, the density gradients caused by the thermal gradients can result in a Rayleigh-Bénard-like instability. Depending on the physical system of interest, either one or both of these causes of instability can be important.

In a recent work [2] the authors considered a problem involving zero and infinite thermal diffusivity with the reacted fluid density being less than that of the unreacted fluid. This corresponds to the instability described in case (1) above. The goal of this work is to consider case (2), when the instability is due solely to thermally induced density gradients, and not to the isothermal density differences of the fluids. Thus in this work we shall assume that at some reference temperature, the densities of the reacted and unreacted fluids are the same; this results in all density differences being due to the temperature gradients near the front.

II. EQUATIONS OF MOTION

The equations governing the propagation of autocatalytic reaction-diffusion fronts have been derived previously [2]. We now review the basic assumptions made in this derivation.

We consider the reaction front to be very thin. Studies have shown the reaction front thickness to be much less than the thermal front thickness (7×10^{-3} cm as compared to 0.5 cm) [2]. This thickness of the reaction front is also small compared to the diameter of the tubes used in these studies, which are typically on the order of 0.1 cm. The thin reaction front approximation can then be justified since this thickness is small compared to the other length scales in the problem. Similar approximations have been used in the study of flame propagation [3–7]. Since we are treating the front as a heat source, conservation of energy requires that the temperature gradient change discontinuously at the front while the temperature itself is continuous.

The other assumption in use involves how the fluid density changes with temperature. Since it is the small density changes due to thermal expansion of the fluids which drives the convective instabilities we are interest in, we can write the fluid density to first order as

$$\rho(T)=\rho_1[1-\alpha(T-T_1)] , \tag{1}$$

where $\rho(T)$ is the density at temperature T, ρ_1 is the density at the reference temperature T_1, and α is the classical thermal expansion coefficient at constant pressure. Such small density changes are included only where they modify gravity.

Under these assumptions, the governing system of equations becomes [2]

$$\frac{\partial \mathbf{V}}{\partial t}+(\mathbf{V}\cdot\nabla)\mathbf{V}=-g\alpha(T_1-T)\hat{\mathbf{z}}-\frac{1}{\rho_1}\nabla P_r+\nu\nabla^2\mathbf{V} , \tag{2a}$$

$$\frac{\partial T}{\partial t}+\mathbf{V}\cdot\nabla T+D_T\nabla^2 T , \tag{2b}$$

$$\nabla\cdot\mathbf{V}=0 , \tag{2c}$$

$$c=\hat{\mathbf{n}}\cdot\hat{\mathbf{z}}\frac{\partial H}{\partial t}-\hat{\mathbf{n}}\cdot\mathbf{V}|_{z=H} , \tag{2d}$$

with jump conditions across the interface between the reacted and unreacted fluids given by

$$[\hat{\mathbf{n}}\cdot\mathbf{V}]_-^+=0 , \tag{2e}$$

$$[\hat{\mathbf{n}}\times\mathbf{V}]_-^+=\mathbf{0} , \tag{2f}$$

$$[P_r]_-^+-[n_i n_j T_{ij}^V]_-^+=0 , \tag{2g}$$

$$[\epsilon_{ijk}n_j n_l T_{kl}^V]_-^+=0 , \tag{2h}$$

$$[\hat{\mathbf{n}}\cdot\nabla T]_-^+=D_T^{-1}\Delta T c , \tag{2i}$$

$$[T]_-^+=0 , \tag{2j}$$

and viscous stress tensor

$$T_{ij}^V=-\nu\rho_1\left[\frac{\partial V_i}{\partial x_j}+\frac{\partial V_j}{\partial x_i}\right] , \tag{2k}$$

where P_r is the reduced pressure given by

$$P_r=P+\rho_1 gz , \tag{3}$$

ν is the kinematic viscosity, D_T is the thermal diffusivity, c is the normal front velocity with respect to the unreacted fluid, H is the vertical position of the front as a function of the horizontal coordinates x and y, and of the time t, $\hat{\mathbf{n}}$ is a unit vector pointing normal to the front into the unreacted fluid, ϵ_{ijk} is the totally antisymmetric tensor defined so that $\epsilon_{123}=\epsilon_{231}=\epsilon_{312}=1$, $\epsilon_{321}=\epsilon_{213}=\epsilon_{132}=-1$, and $\epsilon_{ijk}=0$ otherwise, and where the notation $[\xi]_-^+$ indicates the difference between the values of the quantity ξ on the reacted and unreacted sides of the front. The quantities ν and D_T have been considered constant since experimental data imply negligible temperature corrections to ν and D_T (Ref. [2]).

We shall use length and time scales $D_T c_0^{-1}$ and $D_T c_0^{-2}$ to define dimensionless coordinates $\mathbf{x}^*$ and t^* such that $\mathbf{x}=D_T c_0^{-1}\mathbf{x}^*$ and $t=D_T c_0^{-2}t^*$, where c_0 is the planar front speed. We also define dimensionless dependent variables by

$$T(\mathbf{x},t)=\nu c_0^3 g^{-1}\alpha^{-1}D_T^{-2}\theta(\mathbf{x}^*,t^*) ,$$

$$P_r(\mathbf{x},t)=\rho_1 c_0^2 p(\mathbf{x}^*,t^*) ,$$

$$K(\mathbf{x},t)=c_0 D_T^{-1}\kappa(\mathbf{x}^*,t^*) ,$$

$$\mathbf{V}(\mathbf{x},t)=c_0\mathbf{v}(\mathbf{x}^*,t^*) ,$$

$$H(\mathbf{x},t)=D_T c_0^{-1}h(\mathbf{x}^*,t^*) ,$$

where K is the dimensioned curvature of the front. The dimensionless parameters which are relevant to this problem are the Prandtl number $\mathcal{P}=\nu/D_T$, Lewis number $\mathcal{L}=D_T/D_C$, and Rayleigh number $\mathcal{R}=\alpha g\Delta T D_T^2/\nu c_0^3=\Theta_1-\Theta_0$ for convection driven by the thermal gradients near the front. Typical values for these parameters for the iodate-arsenous-acid system are $\mathcal{R}=898$, $\mathcal{P}=6.34$, and $\mathcal{L}=72.5$ where we have used $c_0=2.95\times10^{-3}$ cm/s, $D_T=1.45\times10^{-3}$ cm^2/s, chemical diffusivity $D_C=2.0\times10^{-5}$ cm^2/s, $\alpha=2.57\times10^{-4}$/°C, and $\nu=9.2\times10^{-3}$ cm^2/s (Ref. [2]). We can now write Eqs. (2) in dimensionless form, with equations of motion

$$\frac{\partial \mathbf{v}}{\partial t}+(\mathbf{v}\cdot\nabla)\mathbf{v}=-\mathcal{P}(\theta_1-\theta)\hat{z}-\nabla p+\mathcal{P}\nabla^2\mathbf{v} , \tag{4a}$$

$$\frac{\partial\theta}{\partial t}+\mathbf{v}\cdot\nabla\theta=\nabla^2\theta , \tag{4b}$$

$$\nabla\cdot\mathbf{v}=0 , \tag{4c}$$

$$\hat{\mathbf{n}}\cdot\hat{\mathbf{z}}\frac{\partial h}{\partial t}=\hat{\mathbf{n}}\cdot\mathbf{v}_-+1+\kappa/\mathcal{L} , \tag{4d}$$

jump conditions

$$[\hat{\mathbf{n}}\cdot\mathbf{v}]_-^+=0 , \tag{4e}$$

$$[\hat{\mathbf{n}}\times\mathbf{v}]_-^+=\mathbf{0} , \tag{4f}$$

$$[p]_-^+=-[n_i n_j T_{ij}^v]_-^+ , \tag{4g}$$

$$[\epsilon_{ijk}n_j n_l T_{kl}^v]_-^+=0 , \tag{4h}$$

$$[\hat{\mathbf{n}}\cdot\nabla\theta]_-^+=\mathcal{R}(1+\kappa/\mathcal{L}) , \tag{4i}$$

$$[\theta]_-^+=0 , \tag{4j}$$

and viscous stress tensor

$$T_{ij}^v=-\frac{\partial v_i}{\partial x_j}-\frac{\partial v_j}{\partial x_i} , \tag{4k}$$

where we have used the eikonal velocity [8] $c=c_0+D_C K$ and we have dropped the asterisks from the dimensionless variables. The unit normal at the front pointing into the unreacted fluid is given by

$$\hat{\mathbf{n}}=\pm\frac{\hat{\mathbf{z}}-\nabla h}{(1+|\nabla h|^2)^{1/2}} , \tag{4l}$$

where the plus sign is used when the unreacted fluid is above the front (upward propagation). This set of equations describes viscous convection for a thin autocatalytic front in the frame of the moving front where the instability is due to thermal effects under conditions such that the reacted and unreacted fluids have the same density at some reference temperature. An eikonal velocity (instead

of activation kinetics) and nonzero viscosity distinguish Eqs. (4) from the equations typically used for flame propagation [3–6]. These equations also differ substantially from a set of equations for viscous flame propagation in a boundary-layer approximation (Ref. [7]).

III. LINEAR STABILITY OF FLAT HORIZONTAL FRONTS

A laterally unbounded system represents the simplest nontrivial geometry in which to study convection for autocatalytic systems. Below we shall develop this calculation for the system when the instability is driven by thermal gradients (as is the case with the classical Rayleigh-Bénard problem). This will result in the calculation of a critical wavelength below which the front is stable to perturbations (resulting in a flat propagating reaction front). This critical wavelength can then be compared with that found when the problem involves a discontinuous density for these autocatalytic systems [2].

The above system of equations has been derived for a coordinate frame fixed to an upward-propagating horizontal front. The location of the unperturbed front is fixed at $z=h=0$. The unreacted fluid is thus in the $z>0$ domain (for upward propagation of the front), while $z<0$ locates the reacted fluid. In this frame, Eqs. (4) yield a steady dimensionless fluid velocity and temperature profile for the undisturbed flat front (with $\kappa=0$):

$$\mathbf{v}^{(0)}=-\hat{\mathbf{z}}\ , \tag{5a}$$

$$\theta^{(0)}=\begin{cases}\theta_0+\mathcal{R}e^{-z}\ , & z\geq 0\\ \theta_1\ , & z<0\ ,\end{cases} \tag{5b}$$

where θ_0 is the dimensionless form of the initial temperature of the unreacted fluid and θ_1 is the dimensionless form of the final temperature of the reacted fluid. Since the dimensionless velocity $\mathbf{v}^{(0)}=-\hat{\mathbf{z}}$ is measured in the moving frame in units of the flat front propagation speed c_0, its value corresponds to zero fluid motion in the laboratory frame. We can now study the linear stability of the flat front by introducing small time-dependent perturbations according to

$$\begin{aligned} h&=h^{(1)}\ ,\\ \mathbf{v}&=\mathbf{v}^{(0)}+\mathbf{v}^{(1)}\ ,\\ \theta&=\theta^{(0)}+\theta^{(1)}\ ,\\ p&=p^{(0)}+p^{(1)}\ ,\end{aligned} \tag{6}$$

with similar expressions for $\hat{\mathbf{n}}$, κ, and T^{v}_{ij}. Substituting these expressions into Eqs. (4) and retaining terms linear in the perturbations yields

$$\frac{\partial\mathbf{v}^{(1)}}{\partial t}+[\mathbf{v}^{(0)}\cdot\nabla]\mathbf{v}^{(1)}=\mathcal{P}\theta^{(1)}\hat{z}-\nabla p^{(1)}+\mathcal{P}\nabla^2\mathbf{v}^{(1)}\ , \tag{7a}$$

$$\frac{\partial\theta^{(1)}}{\partial t}+\mathbf{v}^{(0)}\cdot\nabla\theta^{(1)}+\mathbf{v}^{(1)}\cdot\nabla\theta^{(0)}=\nabla^2\theta^{(1)}\ , \tag{7b}$$

$$\nabla\cdot\mathbf{v}^{(1)}=0\ , \tag{7c}$$

$$\hat{\mathbf{n}}^{(0)}\cdot\hat{\mathbf{z}}\frac{\partial h^{(1)}}{\partial t}=\mathcal{L}\kappa^{(1)}+\hat{\mathbf{n}}^{(0)}\cdot\mathbf{v}_{-}^{(1)}+\hat{\mathbf{n}}^{(1)}\cdot\mathbf{v}_{-}^{(0)}\ . \tag{7d}$$

To obtain useful jump conditions, we must relate the jump conditions at the front, Eqs. (4e)–(4j), to jump conditions which can be imposed at $z=0$, as has been done in similar problems [10]. To do this, we shall, for an arbitrary function ξ, use a Taylor expansion of the form

$$[\xi]_{z=h}=[\xi]_{z=0}+h\left[\frac{\partial\xi}{\partial z}\right]_{z=0}+\cdots\ .$$

Assuming that ξ is of the form $\xi=\xi^{(0)}+\xi^{(1)}$ results in the following jump condition (to first order):

$$[\xi^{(0)}]_{z=h}+[\xi^{(1)}]_{z=h}=[\xi^{(0)}]_{z=0}+[\xi^{(1)}]_{z=0}+h^{(1)}\left[\frac{\partial\xi^{(0)}}{\partial z}\right]_{z=0}\ ,$$

where we have used the fact that $h^{(0)}=0$. Examining this relation we see that the zero-order jump is of the form:

$$[\xi^{(0)}]_{z=h}=[\xi^{(0)}]_{z=0}\ ,$$

with a first-order jump:

$$[\xi^{(1)}]_{z=h}=[\xi^{(1)}]_{z=0}+h^{(1)}\left[\frac{\partial\xi^{(0)}}{\partial z}\right]_{z=0}\ .$$

Applying these results to Eqs. (4e)–(4j) yields

$$[\hat{\mathbf{n}}^{(0)}\cdot\mathbf{v}^{(1)}]_{z=0}=0\ , \tag{7e}$$

$$[\hat{\mathbf{n}}^{(0)}\times\mathbf{v}^{(1)}]_{z=0}=0\ , \tag{7f}$$

$$[p^{(1)}]_{z=0}=0\ , \tag{7g}$$

$$[\epsilon_{ijk}n_j^{(0)}n_l^{(0)}T_{kl}^{v(1)}]_{z=0}=0\ , \tag{7h}$$

$$\left[\frac{\partial\theta^{(1)}}{\partial z}\right]_{z=0}=\mathcal{R}h^{(1)}+\mathcal{R}\kappa^{(1)}/\mathcal{L}\ , \tag{7i}$$

$$[\theta^{(1)}]_{z=0}=-\mathcal{R}h^{(1)}\ , \tag{7j}$$

where

$$T_{ij}^{v(1)}=-\frac{\partial v_i^{(1)}}{\partial x_j}-\frac{\partial v_j^{(1)}}{\partial x_i} \tag{7k}$$

is the perturbation stress tensor and we have used the uniformity of $\mathbf{v}^{(0)}$ to eliminate some terms. We have also used the fact that for two-dimensional perturbations with x, z, and t dependencies and nonzero horizontal and vertical velocity components $u^{(1)}$ and $w^{(1)}$ only, Eq. (4l) implies an undisturbed component of the normal vector $\hat{\mathbf{n}}^{(0)}=\hat{\mathbf{z}}$ and a perturbation component $\hat{\mathbf{n}}^{(1)}=-iqh^{(1)}\hat{\mathbf{x}}$ for upward propagation. Correspondingly, the appropriate curvature

$$\kappa=\frac{1}{(1+|\nabla h|^2)^{1/2}}\frac{d^2h}{dx^2} \tag{8}$$

has a perturbation component $\kappa^{(1)}=-q^2h^{(1)}$. Since Eqs. (7) represent a set of linear homogeneous ordinary differential equations, we can introduce a perturbation wave number q and growth rate σ and endow the perturbations $h^{(1)}$, $\mathbf{v}^{(1)}$, $\theta^{(1)}$, and $p^{(1)}$ with exponential dependencies $e^{iqx+\sigma t}$. By defining $\partial\equiv\partial/\partial z$, we can now use

Eq. (7c) and the horizontal component of Eq. (7a) to obtain

$$u^{(1)}=iq^{-1}\partial w^{(1)} \tag{9a}$$

and

$$p^{(1)}=q^{-2}(\partial^2+\partial-\mathcal{P}q^2-\sigma)\partial w^{(1)}\ , \tag{9b}$$

so that Eqs. (7) yield

$$(\partial^2-q^2)(\mathcal{P}\partial^2+\partial-\mathcal{P}q^2-\sigma)w^{(1)}-q^2\mathcal{P}\theta^{(1)}=0\ , \tag{9c}$$

$$(\partial^2+\partial-q^2-\sigma)\theta^{(1)}-[\partial\theta^{(0)}]w^{(1)}=0\ , \tag{9d}$$

$$w_{-}^{(1)}=(\sigma+q^2/\mathcal{L})h^{(1)}\ , \tag{9e}$$

$$[w^{(1)}]_{z=0}=0\ , \tag{9f}$$

$$[\partial w^{(1)}]_{z=0}=0\ , \tag{9g}$$

$$[\partial^2 w^{(1)}]_{z=0}=0\ , \tag{9h}$$

$$[\partial^3 w^{(1)}]_{z=0}=0\ , \tag{9i}$$

$$[\partial\theta^{(1)}]_{z=0}=\mathcal{R}(1-q^2/\mathcal{L})h^{(1)}\ , \tag{9j}$$

$$[\theta^{(1)}]_{z=0}=-\mathcal{R}h^{(1)}\ . \tag{9k}$$

These equations govern the time evolution of the dimensionless perturbations about a flat front.

This system can be rewritten totally in terms of $w^{(1)}$ by solving Eq. (9c) for $\Theta^{(1)}$ and using this in (9d);

$$[q^{-2}\mathcal{P}^{-1}(\partial^2-q^2)(\mathcal{P}\partial^2+\partial-q^2\mathcal{P}-\sigma)\times(\partial^2+\partial-q^2-\sigma)+\partial\Theta^{(0)}]w^{(1)}=0\ . \tag{10}$$

Requiring the solution to remain bounded as $z\to-\infty$, we find that $w^{(1)}$ is given by

$$w^{(1)}=e^{iqx+\sigma t}(Ae^{\mathfrak{s}_1 z}+Be^{\mathfrak{s}_2 z}+Ce^{\mathfrak{s}_3 z}) \tag{11}$$

for $z<0$, where

$$\mathfrak{s}_1=q\ ,$$

$$\mathfrak{s}_2=-\tfrac{1}{2}+(\tfrac{1}{4}+q^2+\sigma)^{1/2}\ ,$$

$$\mathfrak{s}_3=-\frac{1}{2\mathcal{P}}+\left[\frac{1}{4\mathcal{P}^2}+q^2+\frac{\sigma}{\mathcal{P}}\right]^{1/2}\ .$$

Ahead of the front ($z>0$), the nonuniformity of $\Theta^{(0)}$ requires a solution in the form of a power series of exponentials of the form (again requiring boundedness for large z)

$$w^{(1)}=e^{iqx+\sigma t}\left[\sum_{i=1}^{3}\left[\sum_{k=0}^{\infty}D_k(s_i)e^{-(k+s_i)z}\right]\right]\ , \tag{12}$$

where Eq. (10) implies a recursion relation for the $D_k(s_i)$'s such that

$$D_k(s_i)=\frac{-q^2\mathcal{P}\mathcal{R}D_{k-1}(s_i)}{[(k+s_i)^2-q^2][\mathcal{P}(k+s_i)^2-(k+s_i)-\mathcal{P}q^2-\sigma][(k+s_i)^2-(k+s_i)-q^2-\sigma]}\ , \tag{13}$$

where

$$s_1=q\ ,$$

$$s_2=\tfrac{1}{2}+(\tfrac{1}{4}+q^2+\sigma)^{1/2}\ ,$$

$$s_3=\frac{1}{2\mathcal{P}}+\left[\frac{1}{4\mathcal{P}^2}+q^2+\frac{\sigma}{\mathcal{P}}\right]^{1/2}\ .$$

It is important to note that the above solutions are only valid as long as s_1, s_2 and s_3 are distinct. As soon as any two of these roots become equal or differ only by an integer, this form of the solution is no longer valid. We shall see below that this necessitates care in determining the parameter values for the onset of convection. This will be discussed in more detail below.

If we now assume a form for the position of the front to be

$$h^{(1)}=Ee^{iqx+\sigma t}\ , \tag{14}$$

and use this along with Eqs. (11) and (12) in the jump conditions given above, the problem reduces to a linear algebraic system describing the onset of convection. The system is of the form (after some simplification)

$$\underline{L}U=0\ , \tag{15}$$

where

$$\underline{L}=\begin{bmatrix} a_0 & b_0 & c_0 & 0 & 0 & 0 & -(\sigma+q^2/\mathcal{L}) \\ -a_0 & -b_0 & -c_0 & 1 & 1 & 1 & 0 \\ -a_1 & -b_1 & -c_1 & \mathfrak{s}_1 & \mathfrak{s}_2 & \mathfrak{s}_3 & 0 \\ -a_2 & -b_2 & -c_2 & \mathfrak{s}_1^2 & \mathfrak{s}_2^2 & \mathfrak{s}_3^2 & 0 \\ -a_3 & -b_3 & -c_3 & \mathfrak{s}_1^3 & \mathfrak{s}_2^3 & \mathfrak{s}_3^3 & 0 \\ -a_4 & -b_4 & -c_4 & \mathfrak{s}_1^4 & \mathfrak{s}_2^4 & \mathfrak{s}_3^4 & q^2\mathcal{R} \\ -a_5 & -b_5 & -c_5 & \mathfrak{s}_1^5 & \mathfrak{s}_2^5 & \mathfrak{s}_3^5 & L_{77} \end{bmatrix}\ , \tag{16}$$

$$L_{77}=-q^2\mathcal{R}[(1-q^2/\mathcal{L})+1/\mathcal{P}]$$

and

$$U=\begin{bmatrix} D_0(s_1) \\ D_0(s_2) \\ D_0(s_3) \\ A \\ B \\ C \\ E \end{bmatrix}\ , \tag{17}$$

with

$$a_n = \sum_{k=0}^{\infty} (-1)^n (s_1+k)^n D_k(s_1)/D_0(s_1) , \quad (18a)$$

$$b_n = \sum_{k=0}^{\infty} (-1)^n (s_2+k)^n D_k(s_2)/D_0(s_2) , \quad (18b)$$

$$c_n = \sum_{k=0}^{\infty} (-1)^n (s_3+k)^n D_k(s_3)/D_0(s_3) . \quad (18c)$$

IV. DETERMINING THE VALUES FOR ONSET OF CONVECTION

In order to solve for the onset of convection we must now find those parameter values such that the determinant of the matrix $\underline{L}$ is zero. While this could be done explicitly, it is simpler to calculate the determinant numerically and then find for what values of σ it is zero for any given value of q. The determinant is found by taking the product of the diagonal elements of the LU decomposition of the matrix $\underline{L}$. As was mentioned above, these solutions are only valid as long as s_1, s_2, and s_3 (as well as their counterparts for the solutions when $z<0$) are distinct. An exact analytical treatment of the case of two identical roots requires the addition of new exponential functions into the basis. This can be achieved numerically by separating these identical roots by an arbitrarily small number. An example of when two of these roots coalesce is at the point $\sigma=q$, where $s_1=s_2=q$ and $\det(\underline{L})=0$. Similar difficulties arise if s_1, s_2, and/or s_3 differ only by an integer.

V. RESULTS

Figure 1 shows the growth rate σ versus wave number q for the parameter values $\mathcal{R}=898$, $\mathcal{L}=72.5$, and $\mathcal{P}=6.34$. Trace 1, which represents the mode with the largest growth rate for any wave number, shows that σ is positive for $q<q_c=5.42$. The flat front is stable ($\sigma<0$) for all $q>q_c$, with the largest growth rate σ occurring at a wave number $q_m=1.17$ and a corresponding growth rate $\sigma_m=34.02$.

As discussed above, trace 1 has the largest growth rate for any given wave number and thus represents the experimentally observable state. It corresponds to one set of convective rolls as shown in Fig. 2(a), which is a plot of the velocity field for the parameter values $q=1$ and $\sigma=33.77$, with the perturbed front position shown by a solid trace near $z=0$. This fluid motion results in the temperature enhancements $\theta^{(1)}$ due to the convective

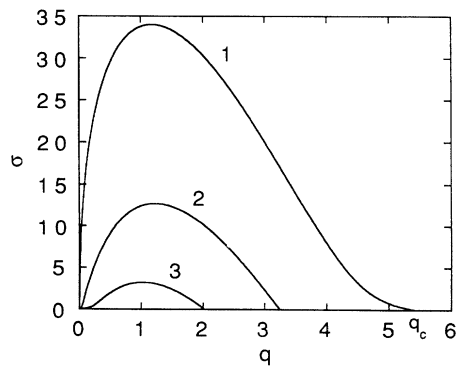

FIG. 1. Dimensionless growth rate σ as a function of dimensionless wave number q for perturbations about an ascending planar autocatalytic reaction front. The wave number q_c is the critical wave number for onset of convection. Traces 1, 2, and 3 correspond to the lowest three modes of the system consisting of one, two, and three sets of rolls, respectively.

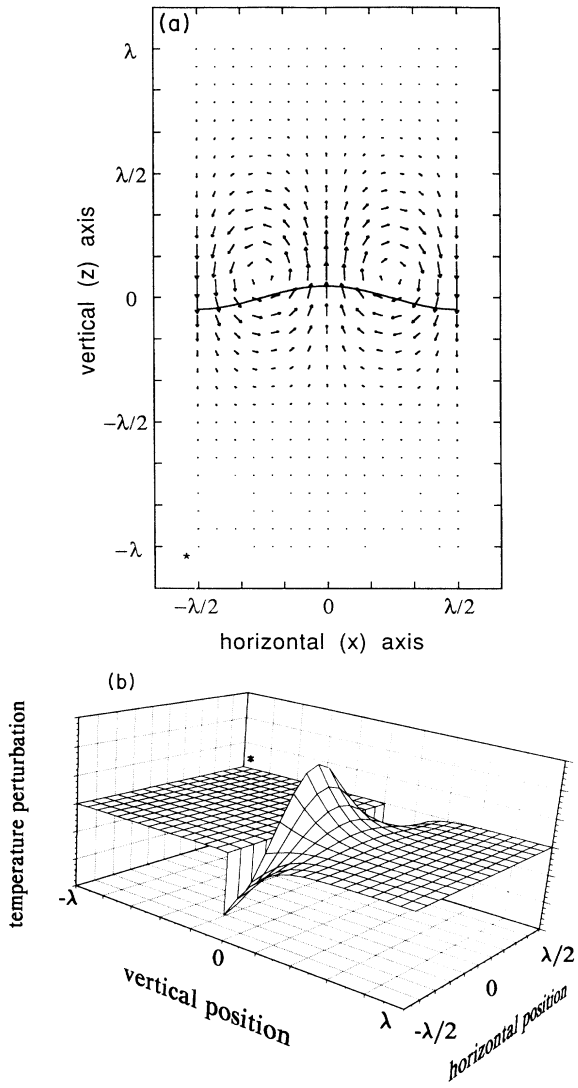

FIG. 2. Convective flow (a) and temperature perturbations (b) arising from the convective flow for $q=1$ showing one set of rolls of wavelength $\lambda=2\pi/q$ and corresponding to trace 1 of Fig. 1. In (a), arrows represent velocity vectors and the solid trace represents the position of the ascending reaction front, with the reacted fluid below the front. Each node in (b) corresponds to a velocity vector in (a), with a reference point denoted by an asterisk. Upflow of the hotter reacted fluid at the origin displaces the reaction front accordingly and enhances the temperature.

fluid motion shown in Fig. 2(b). It should be noted that each velocity vector in Fig. 2(a) corresponds to a node in the grid of Fig. 2(b). The velocity vector labeled with an asterisk in Fig. 2(a) corresponds to the similarly labeled point in Fig. 2(b). As noted before, continuous Θ requires a discontinuous $\Theta^{(1)}$ at $z=0$, which is evident in Fig. 2(b).

Our interest in extending the problem into the nonlinear regime motivates us to study other low-lying modes which will likely play important roles above onset of convection. Trace 2 in Fig. 1 corresponds to two sets of rolls as shown in Fig. 3 with $q=1$ and $\sigma=12.74$, whereas trace 3 in Fig. 1 corresponds to three sets of rolls as shown in Fig. 4 with $q=1$ and $\sigma=3.23$. Investigations have shown there to be a finite number of such curves with positive growth rates. This number is most likely a function of the Rayleigh number.

Figure 5 shows σ versus q plots for various values of

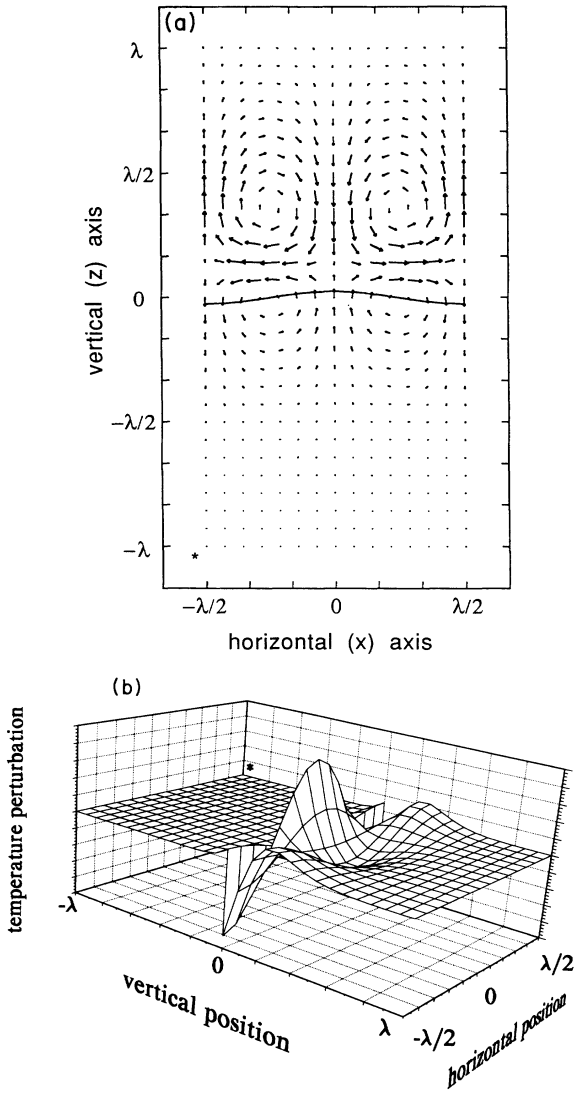

FIG. 3. Convective flow and temperature perturbations for $q=1$ showing two sets of rolls corresponding to trace 2 of Fig. 1.

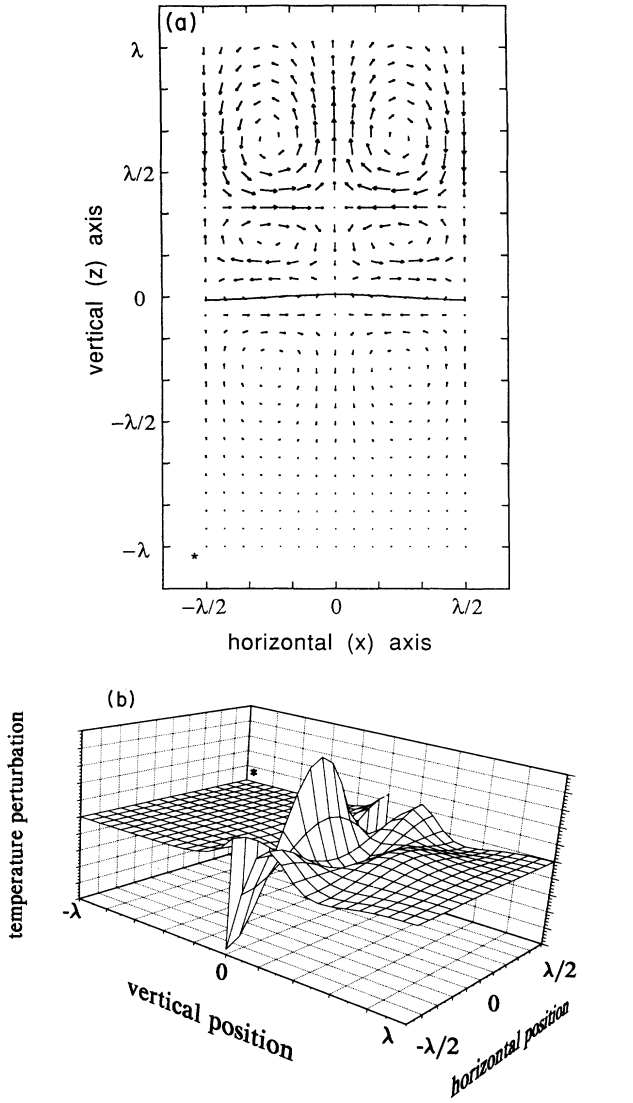

FIG. 4. Convective flow and temperature perturbations for $q=1$ showing three sets of rolls corresponding to trace 3 of Fig. 1.

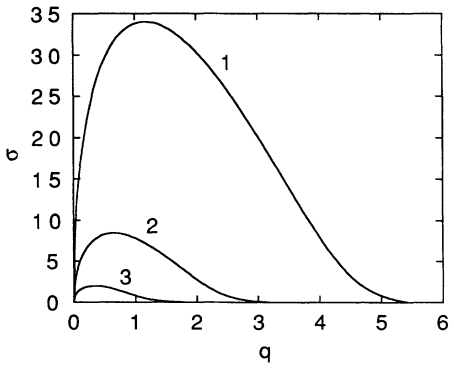

FIG. 5. Dimensionless growth rate σ vs dimensionless wave number q for values of the Rayleigh number $\mathcal{R}=898$, 89.8 and 8.98.

$\mathcal{R}$, with traces 1, 2, and 3 corresponding to $\mathcal{R}=989$ (same as trace 1, Fig. 1), 89.8, and 8.98. This demonstrates that there is no critical Rayleigh number for this system; the propagating front will be unstable over some range of perturbation wavelengths for any concentration of reacting chemicals (i.e., any $\Delta T > 0$).

This growth-rate behavior can be understood heuristically by realizing that finite large wavelengths will always be unstable if the fluid below is lighter than the fluid above because there are no vertical or horizontal boundaries (such as for the Rayleigh-Bénard problem) to preclude these wavelengths. For the Rayleigh-Bénard problem of a laterally unbounded fluid layer heated from below, the growth rate for wavelengths sufficiently large compared to the depth of the layer is negative because the small savings in gravitational potential energy gained by the widely spaced small regions of upflow and downflow cannot balance the cost of maintaining large regions of horizontal flow with their associated viscous dissipation of energy. Thus large wavelengths are effectively precluded by the boundaries in the Rayleigh-Bénard problem. In the present problem, the absence of vertical boundaries implies that the vertical length scale is fixed by the horizontal length scale (the wavelength) rather than by the boundaries, thus allowing large wavelengths.

As can be seen in Fig. 1, trace 1 tails out as it approaches a zero growth rate. A possible explanation of this behavior is the following. Figure 6 shows a typical interface with several normals to the surface drawn in. The instability of the planar front is due to density differences caused by thermal gradients. This leads to the potentially unstable state of a higher density fluid above a lower density fluid. The perturbed interface (Fig. 6) results in additional temperature effects. In the region where the interface is concave down, heat flux in the normal direction tends to diffuse the heat produced by the reaction, while regions where the interface is concave up tend to concentrate the produced heat. This concentration heats the fluid above the front resulting in expansion of the fluid. This heating effect partially counters the effect of the thermal gradients which gave rise to the instability. This effect becomes significant for small wavelengths, where it may produce the observed tail on the σ versus q plot.

Since trace 1 of Fig. 1 represents the lowest mode, we shall use it to estimate the wavelength for onset of convection. The relation between the dimensionless wave number q and the dimensioned wavelength Λ is given by

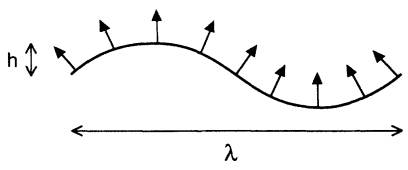

FIG. 6. Schematic diagram of an ascending reaction front (solid trace) and normal vectors pointing into the unreacted fluid (arrows with solid heads) showing the enhanced heat flow into regions where the reaction front is concave up.

$\Lambda = 2\pi D_T c_0^{-1} q^{-1}$. Thus the wavelength for onset of convection for the iodate-arsenous-acid system examined in this work is $\Lambda_c = 0.52$ cm. For $\Lambda < \Lambda_c$ the planar front is stable. The wavelength for onset of convection from the corresponding discontinuous density problem when the thermal diffusivity was assumed to be zero was approximately [2] 0.1 cm, and was approximately 0.13 cm when the thermal diffusivity was assumed to be infinite (Ref. [2]). The implications of the critical wavelengths arising from these two different types of instability may now be discussed. The first type of instability is due to a discontinuous density at the reaction front (neglecting other thermal effects by considering the limits of zero and infinite thermal diffusivity) reminiscent of a Rayleigh-Taylor instability. The second is due to considering a finite, nonzero thermal diffusivity without a jump in density at the interface. This leads to an instability which is driven by thermal gradients similar to those which give rise to the instability in the Rayleigh-Bénard problem. In comparing the relative importance of these two mechanisms leading to instability at the onset of convection, we see that for the previously discussed values of $\mathcal{R}$, $\mathcal{L}$, and $\mathcal{P}$, the observed onset of instability in the physical system where both mechanisms are competing should be governed by the discontinuous density since this results in an instability present at shorter wavelengths than that due to the finite, nonzero thermal diffusivity with continuous density. This further substantiates the conclusion of a recent work [2] by the authors which proposes that in cases where the density behind an ascending front is less than that ahead of the front, the behavior of the system is dominated by the discontinuous jump in density rather than by thermal gradients.

VI. CONCLUSIONS

In light of the above results and the fact that experimental observations show the onset of convection in iodate-arsenous-acid systems to be predicted by the results of the discontinuous density calculations [2], the type of instability studied here should not be of much importance in these systems. This may not be the case for other systems such as Fe(II)-Ni systems where the reacted fluid is more dense than the unreacted fluid (Ref. [9]). In such systems, instability should be governed by thermal gradients. However, detailed experimental observations probing the onset of convection in these systems are required before comparisons can be made. One may also question how the inclusion of the finite thermal diffusivity in the discontinuous density problem will change the character of the solutions obtained from the linear stability analysis. This question is currently under investigation. A further interesting question is the effect of these two types of instability away from onset of convection in the nonlinear regime. These problems are under investigation.

The inclusion of finite thermal diffusivity in the problem of propagating autocatalytic fronts results in a much greater complexity in the solutions than does the corresponding discontinuous density problem. The complexities arise in the solutions being of the form of an infinite

series of exponentials.

The above-described solutions have not been observed experimentally for the arsenous-acid reaction since under experimental conditions used thus far, instabilities similar to those observed in the Rayleigh-Taylor problem due to composition changes result in the onset of convection at smaller wavelengths than those associated with the effects of temperature gradients in the absence of a discontinuous density difference at the interface. The results in this work have fulfilled two major goals. (1) They serve to substantiate the conclusion presented in a previous work on the discontinuous density problem, namely, that at onset of convection the iodate-arsenous-acid system should largely be governed by the discontinuous density difference and not the temperature gradients. (2) They demonstrate how solutions may be obtained when the temperature effects are included and show the nature of these solutions. The above-described onset of convection of systems in which the instability is driven by thermally induced density gradients may be observable in iodate-arsenous-acid systems under appropriate experimental conditions. It may also be relevant to other systems such as Fe(II)-Ni. The results and methods described here will be valuable when the problem including both the density discontinuity and finite thermal diffusivity is studied.

ACKNOWLEDGMENTS

This work was supported in part by the West Virginia University Energy and Water Research Center and by NSF Grant No. RII-8922106.

[1] T. McManus, Ph.D. thesis, West Virginia University, 1989, Chap. 3.
[2] B. F. Edwards, J. W. Wilder, and K. Showalter, Phys. Rev. A **43**, 749 (1991).
[3] L. Landau, Acta Physicochim. URSS **19**, 77 (1944).
[4] Z. Rakib and G. I. Sivashinsky, Combust. Sci. Technol. **54**, 69 (1987).
[5] M. Matalon and B. J. Matkowsky, J. Fluid Mech. **124**, 239 (1982); Combust. Sci. Technol. **34**, 295 (1983).
[6] G. H. Markstein, *Nonsteady Flame Propagation* (Pergamon, Oxford, 1964).
[7] P. Pelce and P. Clavin, J. Fluid Mech. **124**, 219 (1982).
[8] J. J. Tyson and J. P. Keener, Physica D **32**, 327 (1988).
[9] J. A. Pojman, I. P. Nagy, and I. R. Epstein (unpublished).
[10] R. W. Zeren and W. C. Reynolds, J. Fluid Mech. **53**, 305 (1972).